Iranian Journal of Science & Technology, Transaction B: Engineering, Vol. 34, No. B4, pp 433-445
Printed in The Islamic Republic of Iran, 2010

AN INVESTIGATION INTO THE UPWARD AND LATERAL SOIL-PIPELINE INTERACTION IN SAND USING FINITE DIFFERENCE METHOD*

K. BADV** AND K. E. DARYANI

Dept. of Civil Engineering, Urmia University, I. R. of I. R. of Iran
Email: k.badv@urmia.ac.ir

Abstract– Permanent Ground Deformation (PGD), occurring as faulting, liquefaction-induced soil movements and landslides can significantly affect underground lifelines such as buried gas and water pipelines. This paper investigates the response of buried pipelines in sand to transverse PGD with particular attention to the peak forces exerted on the pipe. Available analytical solutions provide a wide range of predicted peak dimensionless forces, but there is limited information regarding the transition of the peak dimensionless force from shallow to deep embedment conditions. There are large uncertainties in the true values since the bounds established by the analytical solutions are large. In order to find the solution and to investigate its failure mechanism, the numerical modeling of soil-pipe interaction is performed for different conditions. The effects of burial depth ratio, pipe size and soil properties are addressed using finite differences analyses. A constitutive model for the continuous strain-hardening/softening and volumetric dilatancy of sand is proposed. The results showed that the transverse soil restraint decreases for larger diameter pipes in the horizontal direction, and there is no effect in the vertical direction. The transverse soil restraint increases with increasing burial depth ratio but it becomes constant at deeper soil profiles.

Keywords– Buried pipelines, earthquake, soil-structure interaction, numerical analysis

1. INTRODUCTION

Extensive damage to lifeline buried pipes has been documented from recent major earthquake disasters. In particular, pipe damage concentrated in the areas of permanent ground deformation resulting from slope failures, earthquake-induced faulting, landslide and liquefaction, urban excavation and tunneling, and excessive ground settlement. Under such circumstances, loads are induced in a pipeline by relative motion between the pipeline and the surrounding soil. In the current state-of-practice (e.g., Committee on Gas and Liquid Fuel Lifelines of ASCE 1984[1]; ALA 2005[2]), the pipeline is generally simplified as a beam, while pipe-soil interaction is represented by soil springs in the axial (or longitudinal), transverse horizontal and vertical directions, as shown in Fig. 1. This simplification is derived from the concept of sub-grade reaction originally proposed by Winkler [3]. Winkler-type soil models are unable to describe complicated soil behavior, such as dilatancy, stress path dependency and, to some extent, strain hardening or softening. The springs describing the soil resistance to deformation are usually assumed independent of one another. Therefore, no connection between adjacent soil zones is considered.

ALA defined the peak transverse yield load (kN/m) per unit length of pipe in sand as follows:

$$P_u = \bar{\gamma} H N_q D \tag{1}$$

*Received by the editors April 14, 2009; Accepted February 17, 2010.
**Corresponding author

Where $\overline{\gamma}$ is the soil effective unit weight; H is the soil depth to the centerline of pipe, D is the pipe outer diameter and N_q is the transverse horizontal or vertical bearing capacity factor adopted from Hansen [4] or Rowe and Davis [5].

Practical engineering solutions, which often use structural finite element (numerical) analysis, are advantageous in terms of the simplicity, functionality and utility for conducting preliminary assessment of pipeline integrity and parametric analysis. The procedures, however, are limited by the underlying assumptions and idealizations considered. Furthermore, analytical difficulties are encountered for pipe-soil interaction events considering non-uniform boundary conditions, spatial variation in characteristics of the pipeline and soil media, large amplitude, accumulated or cyclic deformational loading mechanisms and nonlinear material behavior. For these issues, continuum models using finite element or finite difference methods are robust and comprehensive numerical tools and can address a number of limitations in reproducing soil constitutive behavior, soil deformation mechanisms (e.g. shear load transfer) and soil-pipe interaction (e.g. variable circumferential or longitudinal pressure distribution).

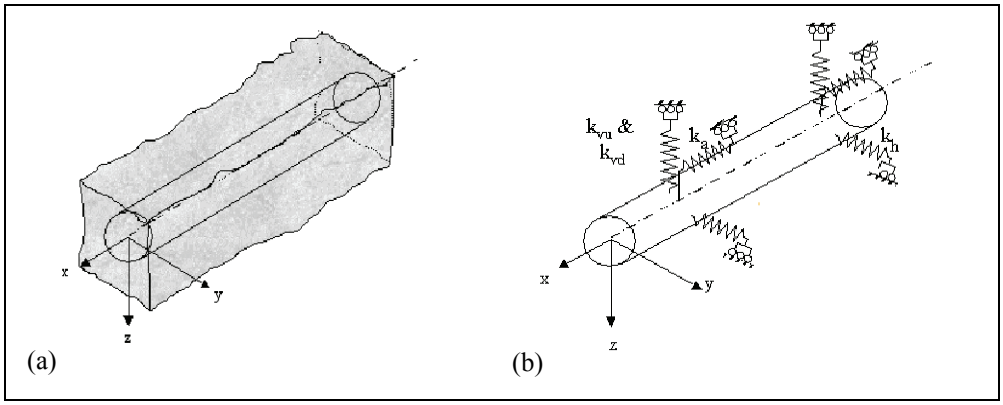

Fig. 1. Soil-pipeline interaction
(a) Continuum analysis model, (b) Idealized structural model [2]

In the finite difference method, the derivatives contained in the governing equations are replaced with algebraic equations written in terms of field variables such as stress, displacement, pore-water pressure, etc. at discrete points. Even though the set of algebraic equations is derived in a different way than that in the finite element method, the two sets of equations are identical. The difference between the two methods is that finite element methods often combine the element matrices into a large global stiffness matrix, where as this is not normally done with finite differences because it is relatively efficient to regenerate the finite difference equations at each step. There are several advantages of FDM, most importantly, no iteration process is necessary when using this method, even if the constitutive law is widely nonlinear.

A number of studies have been conducted to investigate pipe-soil interaction using continuum finite element modeling, including studies conducted by Bruschi et al. [6], Popescu et al. [7] and Nobahar et al. [8].

However, the difficulties in characterizing real soil properties have contributed to the large variation in predicted soil forces and pipe responses, leading to a lack of confidence and limited implementation of numerical modeling in practice. There are few studies with finite difference method. In view of these uncertainties, a review and reappraisal of literature on experimental studies of pipe-soil interaction is conducted. A parametric study based on finite difference method is then performed to provide deeper insight into the understanding of pipe response associated with lateral and upward ground movements. The influences of burial depth, pipe size and soil type to the bearing capacity factors of the surrounding soil were investigated.

2. REVIEW OF PREVIOUS STUDIES

Previous work on soil-pipeline interaction induced by lateral and upward movements mainly focuses on the prediction of the maximum horizontal and vertical soil forces and the force-displacement relations. There are a few publications to describe the effect of some parameters to the loading. More recently O'Rourke and Liu [9] provide detailed reviews of analytical models and experimental tests on transverse soil forces. Only a brief examination of selected experimental studies is given in this paper.

Experimental studies relevant to lateral pipe-soil interaction have been conducted by means of laboratory model tests, centrifuge tests, and in situ full-scale tests. Several early studies were performed using vertical plate anchors to determine limiting states, but the results for plate anchors may not fully reflect the characteristics of buried pipes. Audibert and Nyman [10] tested small diameter pipes ($D = 25 - 114\text{mm}$) in sand for H/D ranging from 1 to 24. Trautmann and O'Rourke [11] performed large-scale tank experiments to investigate the pipeline behavior. The tests were performed for H/D up to 11.5 for lateral loading and H/D up to 13 for upward loading. More recently, a full-scale experimental study was carried out at C-CORE by Hurley et al. [12]. A study that probes pipelines with elbows subjected to PGD was done in the laboratory at Cornell University by Yoshizaki et al. [13]. A centrifuge modeling of PGD response of buried pipe was accomplished by O'Rourke et al. too [14]. The soil restraints to oblique movement of buried pipes in dense sand were investigated by Hsu et al. [15] where model pipes 0.61 m long with diameters of 152.4, 228.6, and 304.8 mm were obliquely moved from an axial-longitudinal to a lateral-transversal direction in a large scale drag box to find the associated longitudinal and transverse soil restraints on the pipes in the shallow buried depth.

As described earlier, numerous numerical researches on interaction between soil and buried pipes have been conducted. The following are examples of such analyses. Altaee et al. [16] performed 2D plane strain analyses of pipes moved laterally through soil. They investigated the performance of various nonlinear soil models implemented in CRISP and AGAC. Popescu and Nobahar [17] studied the effect of groundwater in soil-pipe interaction using ABAQUS/Std. Yimsiri et al. [18] used FEM analyses to investigate soil-pipe interaction at deep embedment conditions and more recently, Guo [19] used the finite element software package ABAQUS/Std for parametric study of buried pipes in clay in order to establish a failure criterion under oblique direction.

3. VALIDATION OF THE NUMERICAL MODEL

The finite difference analysis package, *FLAC 2D* V4.0 (Fast Lagrangian Analysis of Continua), was chosen for the numerical analysis. Since in *FLAC* there is no need to form a stiffness matrix, it is a trivial matter to update coordinates at each time step in large-strain mode. The incremental displacements are added to the coordinates so that the grid moves and deforms with the material it represents. In this 2-D approach, beam elements are used to represent a rigid pipe section and the nodes of the pipe interface elements are attached to the beam nodes to represent the possibility of slippage between the pipe and the soil. Utilizing the intrinsic FISH language allows the developed forces acting on the pipe to be determined directly. The model used in this study was calibrated and validated based on both experimental data and finite element model [20, 21]. Trautmann and O'Rourke [11] conducted experimental tests on buried pipes in sand and their results were used in this study to examine the capability of the current numerical method. Their physical tests were performed in a tank with $1.2(\text{W}) \times 2.3(\text{L}) \times 1.2(\text{D})\text{m}$ dimensions. The schematic of the test set up is shown in Fig. 2.

The Cornell filter sand was used for all tests which were clean, sub-angular, fluvioglacial sand having a coefficient of uniformity (C_u) of 2.6 and an effective grain size (D_{10}) of 0.2 mm. The 102 mm pipe was fabricated from ASTM Grade A-36 steel. Soil–pipe interaction was investigated at three different densities

of 14.8 kN/m^3 (loose), 16.4 kN/m^3 (medium), and 17.7 kN/m^3 (dense), corresponding to a relative density of 0%, 45%, and 80%, respectively.

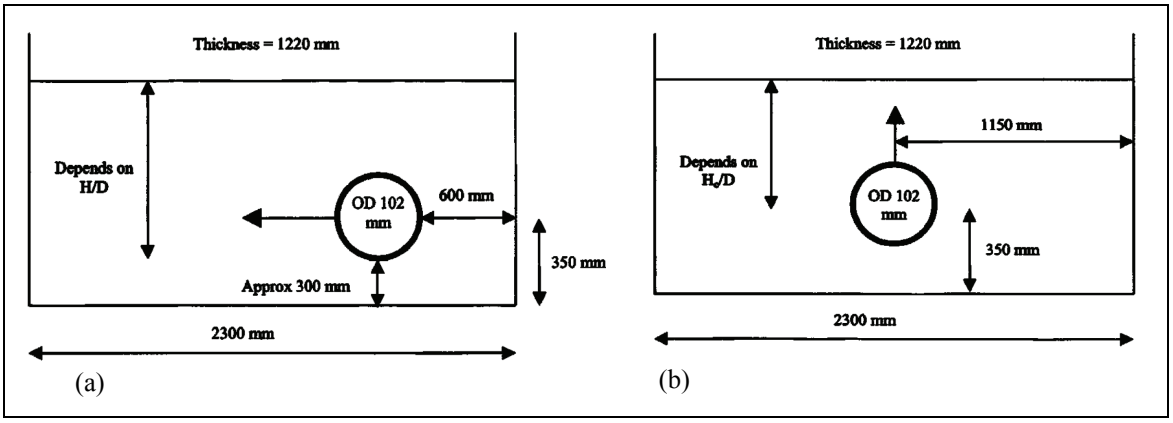

Fig. 2. Schematic of test setup of a large-scale tank
(a) lateral pipe movement, (b) upward pipe movement [11]

In practice, the sand placed around a pipeline is often in a state of medium to dense conditions. Hence, the behavior of these tests in medium and dense sands was simulated using FEM analyses by Yimsiri et al. [18]. Two different soil constitutive models were used in the numerical model; Mohr-Coulomb model, and Nor-Sand model. The results of Nor–Sand were more consistent with the experimental results. In this study, a different constitutive soil model for the continuous strain hardening-softening and volumetric dilatancy of soils is proposed using finite difference method to simulate the nonlinear behavior of sand. The soil-pipe interaction analyses are conducted for two different burial depths in dense sand; H/D=2 and 11.5 for lateral movement and H/D=4 and 13 for upward movement.

4. STRAIN-HARDENING/SOFTENING CONSTITUTIVE MODEL

This model is based on the Mohr-Coulomb model with non-associated shear and associated tension flow rules. The differences, however, lie in the possibility that the cohesion, friction, dilation and tensile strength may harden or soften after the onset of plastic yield. In the Mohr-Coulomb model those properties are assumed to remain constant. Four parameters are needed to create this model, namely the elastic modulus E, bulk modulus B, yield function f, and plastic potential function g.

Using the concept of the Hyperbolic Model recommended by Duncan and Chang [22], the relation between deviatoric stress and axial strain is similar to a hyperbolic curve when the axial strain is smaller than 0.5% to determine the elastic modulus E [22]. According to the theory of elasticity, the value of bulk modulus can be expressed as a function of elastic modulus (E) and Poisson's ratio (v).

A yield function f is needed for the continuous strain-hardening and strain-softening behavior of soil. Since the Mohr-Coulomb yield criterion is a function of the mobilized friction angle ϕ^*, the yield criterion can be expressed as follows:

$$\sin\phi^* = \frac{\sigma_1 - \sigma_3}{\sigma_1 + \sigma_3} \tag{2}$$

Therefore, the yield function f can be drawn as

$$f = \sigma_1 - \sigma_3 \frac{1 + \sin\phi^*}{1 - \sin\phi^*} \tag{3}$$

The mobilized friction angle ϕ^* is a function of accumulative plastic strain ε^p. According to Vermeer and deBorst [21], during the strain-hardening stage, the relationship between mobilized friction angle ϕ^*, and accumulative plastic strain ε^p can be written as [23]:

$$\phi^* = \sin^{-1}\left(\frac{2\sqrt{\varepsilon^p \times \varepsilon_f^p}}{\varepsilon^p + \varepsilon_f^p}.\sin\phi_p\right) \tag{4}$$

Where ε_f^p is the accumulative plastic strain at peak deviatoric stress, ϕ_p is the peak friction angle of soil. When soil is stressed into a strain softening stage ($\varepsilon_f^p < \varepsilon^p$), the mobilized friction angle ϕ^* decreases from ϕ_p to ϕ_{cv} as the accumulative plastic strain increases. According to Hsu [24], this study proposes the following equation to describe the strain softening behavior :

$$\phi^* = \phi_{cv} + (\phi_p - \phi_{cv}) \times \exp\left[-\left(\frac{\varepsilon^p - \varepsilon_f^p}{\varepsilon_c^p}\right)\right] \tag{5}$$

Where ε_c^p is the strain softening parameter, and ϕ_{cv} is the constant volume friction angle.

As described earlier, the yield function, *f*, is the Mohr-Coulomb yield criterion and is related to the accumulative plastic strain. Assuming the yield function is a plastic potential function *g*, it can be used to describe the dilating behavior of cohesionless soil. Since there is some energy dissipation during shearing, the direction of plastic strain increment tensor $d\varepsilon_{ij}^p$ is not perpendicular to the yield surface. So a plastic potential, function *g*, is required to describe the relationship between plastic strain increment tensor $d\varepsilon_{ij}^p$ and stress tensor ε_{ij}. In other words, a non-associated flow rule exists between the plastic strain increment and the stress tensor of these two cohesionless soils. The plastic potential function, *g*, is similar to the yield function, *f*, and can be expressed as the following equation:

$$g = \sigma_1 - \sigma_3 \frac{1 + \sin\psi^*}{1 - \sin\psi^*} \tag{6}$$

Where ψ^* is mobilized dilatancy angle.

According to the stress-dilatancy theory recommended by Rowe, when tested under a triaxial compression condition, the mobilized dilatancy angle ψ^* for the dilating soil can be represented by an equation of the form:

$$\psi^* = \sin^{-1}\left(\frac{\sin\phi^* - \sin\theta}{1 - \sin\phi^* \sin\theta}\right) \tag{7}$$

Where θ is the dilatancy parameter [25]. The relationships among ψ^*, ϕ^* and θ development with ε^p are shown in Fig. 3 and can be explained as follows:

1. When ε^p is smaller than the accumulative plastic strain at initial dilatancy, ε_d^p, no dilation occurs, so the mobilized dilatancy angle $\psi^* = 0$, and

$$\theta = \phi^* \tag{8a}$$

2. When $\varepsilon_d^p \le \varepsilon^p < \varepsilon_f^p$,

$$\theta = \phi_d^* + 2(\phi_{cv} - \phi_d^*)\left(\frac{\sqrt{(\varepsilon^p - \varepsilon_d^p)}(\varepsilon_f^p - \varepsilon_d^p)}{(\varepsilon^p - \varepsilon_d^p) + (\varepsilon_f^p - \varepsilon_d^p)}\right) \tag{8b}$$

3. When $\varepsilon^p \ge \varepsilon_f^p$,

$$\theta = \phi_{cv} \tag{8c}$$

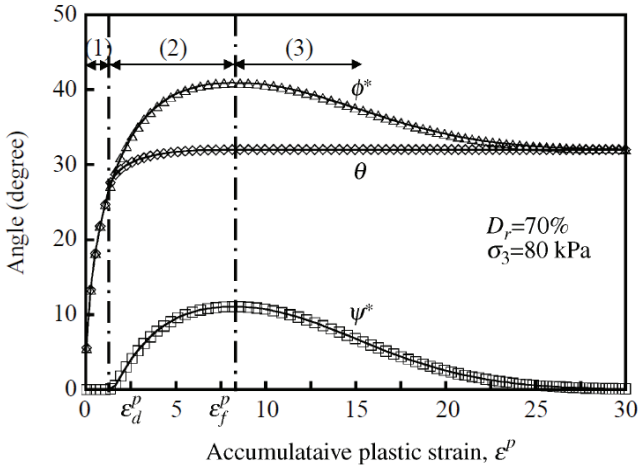

Fig. 3. Relationship among ψ^*, φ^* and θ versus ε_p of dense sand [24]

Where ε_d^p is the accumulative plastic strain at initial dilatancy, which can be determined from triaxial test results, and ϕ_d^* is the mobilized friction angle at initial dilatancy [26]. Using ε_d^p to replace ε^p, and substituting for ε_d^p into Eq. (4) leads to

$$\phi_d^* = \sin^{-1}\left(\frac{2\sqrt{\varepsilon_d^p \times \varepsilon_f^p}}{\varepsilon_d^p + \varepsilon_f^p}.\sin\phi_p\right) \tag{9}$$

The above parameters can be obtained from triaxial test results. Hsu [24] showed that all the above parameters can be derived as a function of D_r and σ_3.

To simulate the experimental soil-pipe model, some of the actual parameters reported by Trautmann and O'Rourke [11] were used. The parameters of D_r = 80%, γ = 17.7 kN/m^3 were used for dense sand were then adjusted to conform to the effective vertical stress σ_v' at the center of the pipe for upward pipe movement, for each case of embedment depth. The input parameters are summarized in Table 1.

Table 1. Input softening/hardening parameter values used for soil-pipe Interaction in lateral and upward directions

Direction	Lateral		Upward	
Embedment ratio (*H/D*)	2	11.5	4	13
B (kPa)	5.26×10^3	7.46×10^3	6.04×10^3	7.64×10^3
G (kPa)	0.63×10^3	2.54×10^3	1.09×10^3	2.80×10^3
ϕ_p	44	44	44	44
ϕ_{cv}	31	31	31	31
ε_f^p	0.001	0.001	0.01	0.01
ε_c^p	0.035	0.088	0.025	0.066
ε_d^p	0.000	0.000	0.000	0.000

5. FDM SETUP AND NUMERICAL ANALYSIS PROCEDURE

The example of fine mesh used for the analyses is shown in Fig. 4. The analysis is performed in plane strain and dry conditions. The distance between boundaries is chosen large enough to eliminate the boundary effect. A displacement boundary fixed in x direction is provided on both sides of the grid and a rigid displacement boundary (fixed in x and y directions) is provided at the bottom of the grid. By setting initial conditions in the *FLAC* grid, an attempt is made to reproduce this in-situ state so that the soil domain is initially equilibrated to gravity stresses. The interaction between the pipeline and surrounding soil is modeled by an interface element, in which the slip and separation between the pipe and soil is allowed. The pipe is pulled in the lateral and upward directions by imposing displacement boundary conditions to all nodes of the pipe; hence, there is no nodal rotation in the pipeline section due to rigid behavior.

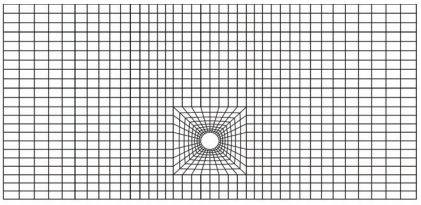

Fig. 4. An example of finite difference mesh of soil-pipe interaction model

The interface friction angle between the pipe and soil, ϕ_m, is assumed to be equal to $\phi_p / 2$. In fact, this parameter is not easy to evaluate because it depends on the interface characteristics and the degree of relative movement (slip) between the pipe and soil. Generally, the pipe surface friction angle ϕ_m ranges from about 20° to a value equal to the friction angle of the soil [27]. The larger values would be the characteristic of rough uncoated pipes with rusty or corroded surfaces and the lower values would correspond to pipes with a smooth coating. Some FDM analysis results are shown in Figs 5 and 6 in the form of force–displacement curves for lateral and upward pipe movements, respectively.

For lateral pipe movement, at *H/D* of 2 and 11.5, the FDM results agree both with the experimental data and FE results for dense sand (Figs. 5a and 5b), whereas they underestimate the experimental data for medium sand.

For upward pipe movement, at *H/D* of 4 and 13, the FDM results are in good agreement with the experimental data and FE results for dense sand (Figs. 6a and 6b), whereas they underestimate the experimental data for medium sand.

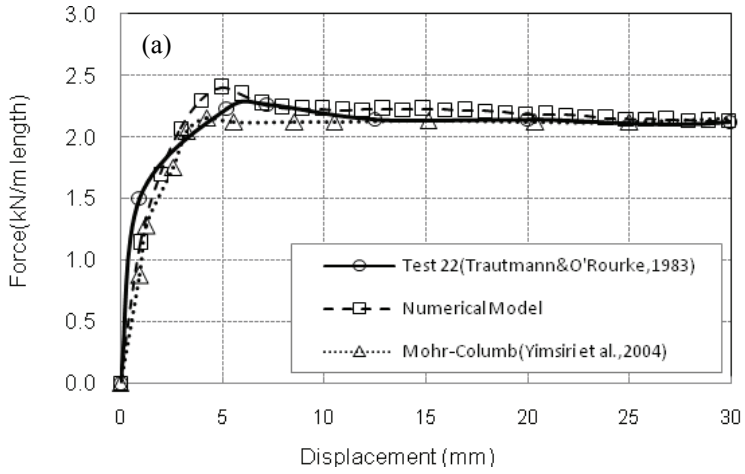

Fig. 5. Results of analysis for lateral pipe movement, (a) H/D=2, (b) H/D=11.5

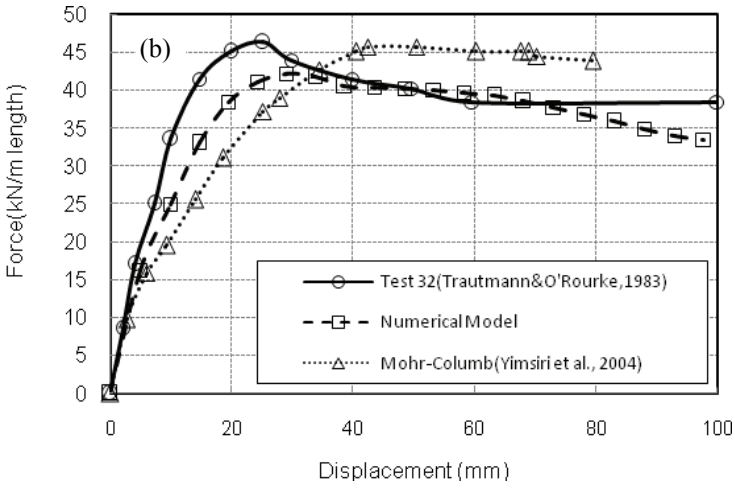

Fig. 5. Continued.

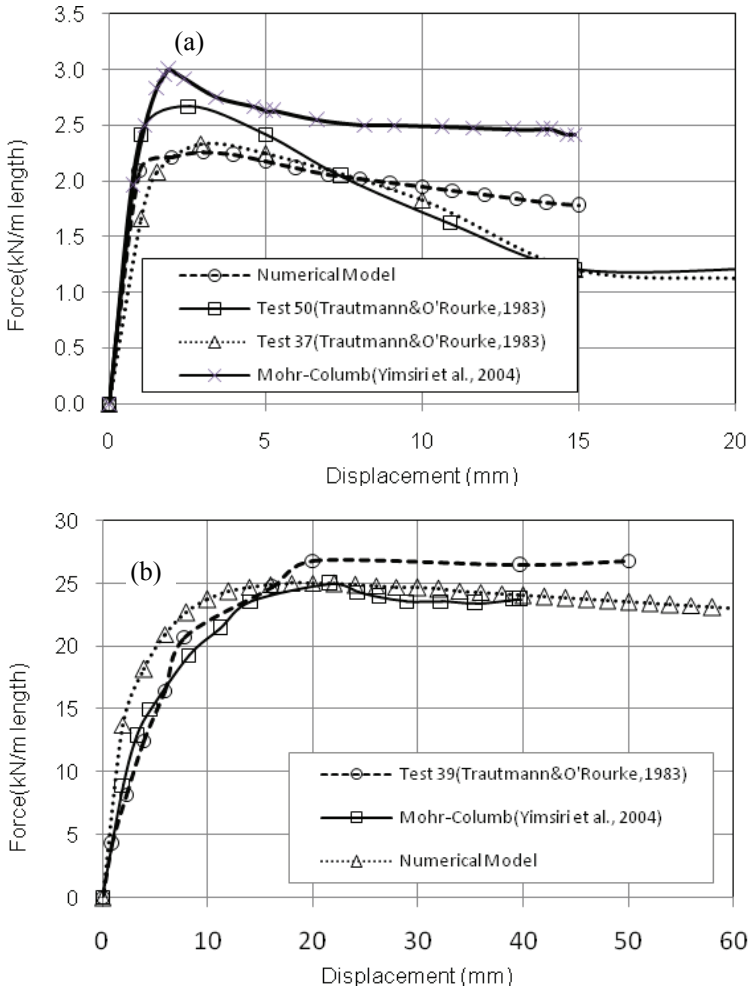

Fig. 6. Results of analysis for upward pipe movement, (a) H/D=4, (b) H/D=13

6. PARAMETRIC ANALYSIS AND DISCUSSION OF RESULTS

This section addresses the scale effect and the influence of burial depth corresponding to various series of models. The influence of soil properties, including dilatancy, strain hardening and pressure dependency, is investigated by changing the parameters used in the soil model.

a) Scale effects of pipe diameter

To study the scale effects of pipe diameter on the dimensionless ultimate transverse bearing capacity, N_q, the results of the analysis for different pipe sizes at the same burial depth (H/D=5) were grouped together as shown in Figs. 7a and 7b for both horizontal and vertical directions buried in medium sand ($\phi_p = 40^\circ, \gamma_d = 15\ kN/m^3$).

As shown in Figs. 7a and 7b, the maximum horizontal dimensionless force, N_{qh}, at a given burial depth ratio varies with pipe diameter D, but it was found that the changes of the maximum vertical dimensionless force, N_{qv}, are minor and can be neglected. More specifically, N_{qh} decreases from 13.7 to 9.8 when D increases from 0.3 to 2 and N_{qv} changes from 3.9 to 4.1 at H/D=5.

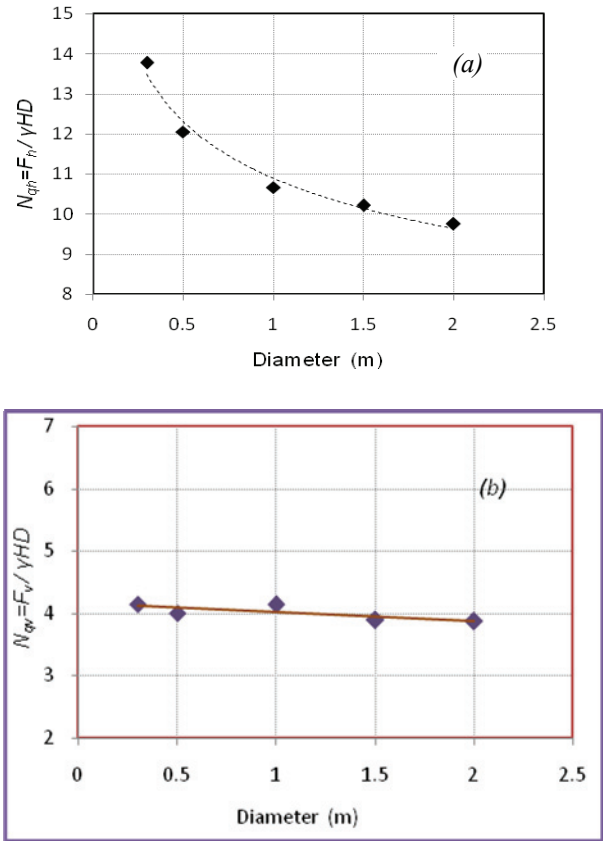

Fig. 7. Values of bearing capacity factor for various pipe sizes,
(a) horizontal direction, (b) vertical direction

b) Effects of burial depth ratio

After calibrating the FDM models with the tank experiments as well as the FEM models, pipe loading cases were simulated using the input parameters derived for the various embedment ratios. An example of the computed force-displacement curves are shown in Fig. 8 in the case of medium sand ($\phi_p = 40^\circ, \gamma_d = 15\ kN/m^3$) where pipe diameter is D=1 m.

Figure 8 shows the relationship between the peak dimensionless force per unit length of pipe and embedment ratio obtained from the analyses. It is found that the predicted interaction forces increases where burial depth ratio increases or the height of backfill increases. Also, for a given pipe diameter D, with the increase of H/D ratio, a larger pipe displacement is required to mobilize the maximum soil resistance. The relation of N_{qh} with burial depth ratios is plotted in Fig. 9. As maintained on the graph, the value of N_{qh} increases with H/D at shallow conditions ($H/D<10$).

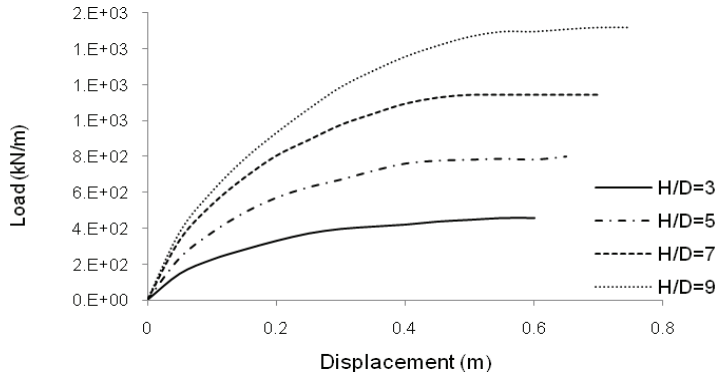

Fig. 8. Horizontal force-displacement curve for different burial depth ratios in the medium sand ($D=1m$)

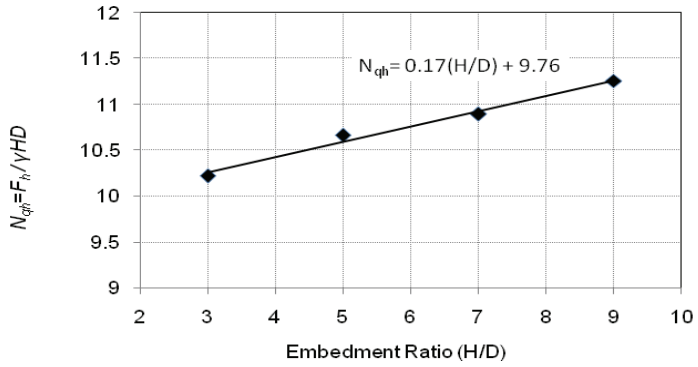

Fig. 9. Function of horizontal maximum dimensionless forces versus different burial depth ratios in the medium sand ($D=1m$)

At deeper depths, the displacement pattern of medium sand shows local shear failure around the pipe, therefore the failure mechanism is different from that at shallow depths. In order to investigate the effect of burial depth on pipe–soil interactions in the case of deep conditions, the analysis extended to larger *H/D*. The results of analysis to estimate the dimensionless horizontal bearing capacity factor, N_{qh}, from *H/D*=3 to 60 for a rigid pipe *D*=200 mm were produced. Four different cases of sandy soil were proposed for higher *H/D* ratios. Table 2 shows a summary of sand properties.

Table 2. Properties of sand used in the analyses for higher *H/D* ratios

Case No.	$\rho(kg/m^3)$	ϕ	ψ	$E(MPa)$
1	1317	32	0	6
2	1500	36	5	15
3	1543	40	10	20
4	1700	44	15	22

Figure 10 shows the dimensionless horizontal bearing capacity factor, N_{qh}, plotted against embedment ratios of as large as 60. The results show that, for transverse pipe movements, the peak dimensionless forces increase approximately linearly with the embedment ratios at shallow embedment conditions and reach their maximum values at a certain embedment ratio, after which the peak dimensionless forces are approximately constant. The depth at which this transition occurs is called the "critical embedment depth" and the constant peak dimensionless force is termed the "critical peak dimensionless force". For lateral

pipe movement, the critical embedment ratio for dry sand is *H/D*=15 with the corresponding critical peak dimensionless force of 9 to 20. In all analyses, since the shearing resistance of soil is a function of confining pressure which varies with burial depth, the softening/hardening soil model is more applicable.

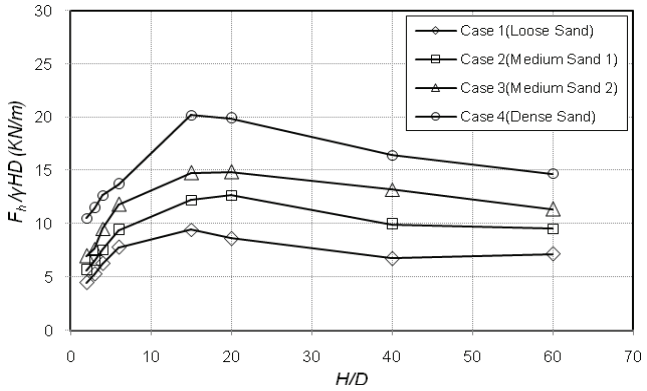

Fig. 10. Variation of maximum dimensionless forces with burial depth ratio in the case of deep conditions for sands

c) Effects of soil type

It is known that shear-induced volume change, or dilatancy, and strain hardening and stress level play an important role in the strength and deformation behavior of granular soils. Thus, one should expect that these soil properties affect the pipe–soil interaction induced by lateral soil movement.

The effect of soil dilatancy on pipe–soil interaction is investigated. The analyses are conducted at three different densities; 14.6 kN/m^3 (loose, $\phi_p = 32^\circ$), 15 kN/m^3 (medium, $\phi_p = 40^\circ$), and 16.1 kN/m^3 (dense, $\phi_p = 44^\circ$) which corresponded to the relative density of 30%, 50%, and 70%, respectively. Figure 11 shows the force-displacement curve where pipe diameter is *D*=1 m and *H/D*=5.

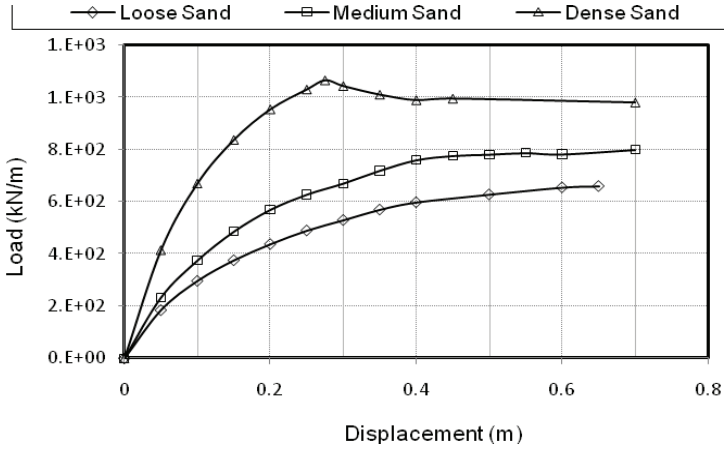

Fig. 11. The effect of soil properties on force–displacement curves of soil-pipe interaction in lateral direction, D=1 m, H/D=5

Figure 11 shows the effect of sand type on force-displacement of pipelines buried at the same conditions. The results show that, the maximum normal force per unit length depends on the type of soil surrounding the pipe (i.e., the compaction control of the backfill). Pipes buried in dense sand have a stiffer response, so the exert force decreases at larger soil movements. However, the values of normal force for pipes buried in loose sand are less than dense sand. It is concluded that the dimensionless bearing capacity factor, N_q, increases with the relative density of soils.

7. SUMMARY AND CONCLUSIONS

The results of the analyses of soil restraint to the transverse movement of pipes in sand were presented. The results of the nonlinear Mohr-Coulomb model to predict the soil restraints to the transverse movement of pipes were presented together with the experimental results. The summary and conclusions of this study are as follows:

1. The soil-pipeline interaction numerical analysis was performed using finite difference method. The predictive capability of strain-softening/hardening constitutive model on sand was demonstrated.
2. The method of lateral interaction is introduced, the pipeline moves against the soil or the soil moves against the pipeline. This affects the stresses and strains and consequently, affects the magnitude of lateral and vertical interaction force as a function of the soil type, pipe size and embedment depth of buried pipe.
3. Based on the parametric study, the variation of the maximum dimensionless force N_q with pipe diameter D and burial depth ratio H/D was established.
4. The variation of bearing capacity factor in the horizontal component is a function of the pipe diameter. Therefore, for a given burial depth ratio, a pipe with a smaller diameter has a larger ultimate horizontal dimensionless force with no changes in the vertical component observed.
5. Although N_q increases with H/D at shallow conditions, the relation is not unique for all depths. Because of the local failure mechanism at large H/D, the variation of N_q is assumed to be zero at deep conditions for pipes buried in sand in both lateral and vertical directions.
6. For a given burial depth ratio H/D and a given pipe diameter D, a larger ultimate horizontal dimensionless force, and therefore a stiffer response were produced at smaller relative pipe displacement in dense sand than in loose sand. Therefore, for pipes buried in sand, an increase of N_{qh} value was observed with the increase in soil dilatancy.

REFERENCES

1. TCLEE. (1984). Guidelines for the seismic design of oil and gas pipeline systems. *ASCE*, Committee on gas and liquid fuel.
2. American Lifeline Alliance (ALA). (2005). Seismic guidelines for water pipelines. "www.americanlifelinealliance.org".
3. Winkler, E. (1867). *Die leher von der elastizitat und festigkeit. dominicus Prague. Dominicus*, Prague.
4. Hansen, J. B. (1961). The ultimate resistance of rigid piles against transversal forces, *Bulletin No. 12, Danish Geotechnical Institute*, Copenhagen, Denmark, pp. 5–9.
5. Rowe, R. K. & Davis, E. H. (1982). The behavior of anchor plates in sand. *Geotechnique*, Vol. 32. No. 1, pp. 25–41.
6. Bruschi, R., Monti, P., Bolzoni, G. & Tagliaferri, R. (1995). Finite element method as numerical laboratory for analyzing pipeline response under internal pressure. axial load, bending moment, *Proceeding of 14th Offshore Mechanics and Arctic Engineering*, OMAE, Houston, TX, USA, Vol. 5, Pipeline Technology, pp. 389-401.
7. Popescu, R., Philips, R., Konuk, I. & Deacu, D. (1999). Numerical and physical modeling of pipe-soil interaction. *Proceedings of the 52nd Canadian Geotechnical Conference*, Regina, SK, pp. 437-444.
8. Nobahar, A., Popescu, R. & Konuk, I. (2000). Estimating progressive mobilization of soil strength. *Proceeding of 53rd Canadian Geotechnical Conference*, pp. 1311-1317.
9. O'Rourke, M. J. & Liu, X. (1999). *Response of buried pipelines subject to earthquake effects,* MCEER Monograph No. 3.

10. Audibert, J. M. E. & Nyman, K. J. (1977). Soil restraint against horizontal motion of pipes. *Journal of Geotechnical Engineering Division, American Society of Civil Engineers*, Vol. 103, No. 10, pp. 1119–1142.
11. Trautmann, C. H. & O'Rourke, T. D. (1983). *Behavior of pipe in dry sand under lateral and uplift loading*, Geotechnical Engineering Report 83-7, Cornell University, Ithaca, N. Y.
12. Hurley, S. & Phillips, R. (1999). *Large scale modeling of pipeline/soil interaction under lateral loading.* Final Report. Contract Report for Minerals Management Service, U.S. Department of the Interior, C-CORE Publication, p. 225.
13. Yoshizaki, K. & Sakanoue, T. (2004). Analytical study on soil-pipeline interaction due to large ground deformation, *13th World Conference on Earthquake Engineering*, Vancouver, B.C., Canada, Paper No. 1402.
14. O'Rourke, M., Gadicherla, V. & Abdoun, T. (2005). Centrifuge modeling of PGD response of buried pipe. *Journal of Earthquake Engineering and Engineering Vibration,* Vol. 4, No. 1, pp. 69-73.
15. Hsu, T., Chen, Y. & Hung, W. (2006). Soil restraint to oblique movement of buried pipes in dense sand. *J. Trans. Eng*., Vol. 132 No. 2, pp. 175–181.
16. Altaee, A. & Boivin, R. (1995). Laterally displaced pipelines: finite element analysis. *Proceedings of 14th International Conference on Offshore Mechanics and Arctic Engineering*, Vol. 5, pp. 209-216.
17. C-CORE. (2003). *3D finite element analysis of pipe-soil interaction – effects of groundwater*. Final Report Prepared for Minerals Management Service, C-CORE Report R-02-029-076.
18. Yimsiri, S., Soga, K., Yoshizaki, K., Dasari, R.G. & O'Rourke, T. D. (2004). Lateral and upward soil-pipeline interactions in sand for deep embedment conditions. *ASCE Journal of Geotechnical Engineering,* Vol. 130, No. 8, pp. 830–842.
19. Guo, P. G. (2005). Numerical modeling of pipe-soil interaction under oblique loading. ASCE *Journal of Geotechnical Engineering,* Vol. 131 No. 2, pp. 260–268.
20. Hataf, N. & Razavi, M. R. (2003). Model tests and finite element analysis of bearing capacity of ring footing on loose sand. *Iranian Journal of Science and Technology, Transaction B: Engineering*, Vol. 27, No. B1, pp. 47-56.
21. Lashkari, A. (2009). A constitutive model for sand liquefaction under rotational shear. *Iranian Journal of Science and Technology, Transaction B: Engineering*, Vol. 33, No. B1, pp. 31-48.
22. Duncan, J. M. & Chang, C. Y. (1970). Nonlinear analysis of stress and strain in soils. *Journal of Soil Mechanics and Foundations Division, ASCE*, Vol. 96, No. SM5, pp. 1629-1653.
23. Vermeer, P. A. & de Borst, R. (1984). Non-associated plasticity for soils, concrete and rock. *Heron*, Vol. 29, No. 3, pp. 5-64.
24. Hsu, S. T. (2005). A constitutive model for the uplift behavior of anchors in cohesionless soils. *Journal of the Chinese Institute of Engineers*, Vol. 28, No. 2, pp. 305-317.
25. Ryan, G. N., Noori, M. & Hou, Z. (1997). Performance of response spectrum generation methods in earthquake engineering. *Iranian Journal of Science and Technology, Transaction B: Engineering*, Vol. 21, No. 3, pp. 299-308.
26. Hataf, N. & Agha Ebrahimi, S. (1999). A degradation model for the triaxial cyclic loading behavior of Shiraz silty clay. *Iranian Journal of Science and Technology, Transaction B: Engineering*, Vol. 23, No. 1, pp. 65-73.
27. Yoshima, Y. & Kishida, T. (1981). A ring torsion apparatus for evaluating friction between soil and metal surfaces. *Geotechnical Testing Journal, ASTM*, Vol. 4, No. 4, pp. 145–152.